

Direct Electrochemistry of Glucose Oxidase on a Graphene-Graphene Oxide Nanocomposite-Modified Electrode for a Glucose Biosensor

Bo Wang¹, Xiaoli Wang², Zhifang He¹, Xiufeng Zhao², Linyu Wang¹

¹ Hebei Key Laboratory of Heterocyclic Compounds. School of chemical engineering & materials, Handan University, Handan, 056005, PR China.

² Department of medicine, First Hospital of Handan City, Handan, 056005, PR China.

*E-mail: hdxyxb@hdc.edu.cn

Received: 5 April 2019 / Accepted: 20 May 2019 / Published: 30 June 2019

Direct electrochemistry of glucose oxidase (GOD) was conducted on the surface of a novel graphene-graphene oxide (GR-GO) nanocomposite. GR-GO possesses the virtues of excellent biocompatibility and conductivity, and high sensitivity to local perturbations, and can provide a biocompatible microenvironment for protein immobilization and a suitable electron transfer distance between the electroactive centers of GOD and the electrode surface. The voltammetric results indicated that GOD assembled on GR-GO retained its native structure and bioactivity, exhibited a surface-confined process, and underwent an effective direct electron transfer (DET) reaction with an apparent rate constant (k_s) of 3.5 s^{-1} . Furthermore, the proposed biosensor exhibited a wider linear response to glucose concentrations between 0.1 mM and 11 mM, with a detection limit of 20 μM and a much higher sensitivity ($15.85 \mu\text{A mM}^{-1} \text{ cm}^{-2}$).

Keywords: direct electron transfer, graphene, graphene oxide, glucose oxidase

1. INTRODUCTION

Because glucose is constantly monitored in the treatment of diabetes, therefore, it is essential to understand determination of glucose concentration rapidly and accurately. There is great interest in biological sensors that are precise with fast response ability, convenient operation, portable, and do not damage the samples or the environment [1]. Clark and Lyons [2] proposed the concept of glucose enzyme electrodes in 1962 for the detection of glucose, and since then, the third generation of glucose biosensors based on the direct electrochemistry of glucose oxidase (GOD) has been developed [3,4]. The third generation of glucose biosensors possess the advantageous of achieving direct electron

transfer (DET) between a redox enzyme and an electrode, which allows one to work out the complex problems associated with using expensive, toxic, unstability redox mediators [5]. In addition, an in-depth study of electrochemistry of redox enzymes/proteins can also lay the foundation for further understand the mechanisms of electron transfer in biological systems [6,7]. On account of the active site (the flavin adenine dinucleotide (FAD)) of GOD is hidden by protective protein shell deeply, and further hindered DET of GOD. That limit the development of the third generation glucose biosensor through [3].

Thus far, in order to obtain the better performance glucose biosensor, and various methods have been made to improve the DET between the redox-active sites of GOD and the electrode surface. A variety of materials, comprising polymers [8,9], metal or metal oxide nanoparticles [10-12], ionic liquid [13,14], and carbon nanotubes [15,16] have already been employed to modify electrodes for immobilizing GOD and further facilitating the DET. A great deal of research has been conducted involving graphene and graphene-based hybrid materials [17-20] because they are very versatile. All these findings obviously demonstrate that it is essential to choose an immobilization matrix with good electrical conductivity, stability, and antifouling property biosensor applications.

Currently, graphene (GR), as a two-dimensional sheet of sp^2 -bonded carbon atoms perfectly arranged in a honeycomb lattice [21], which possesses large ratio of surface area, excellent electrical conductivity, and high electrocatalytic activity than the traditional materials. Due to these properties, GR has many potential applications in supercapacitors [22], batteries [23], nanocomposites [24], and biosensors [17,18]. However, GR sheets tend to form graphite by restacking due to the van der Waals force of attraction. Hence, it is difficult to display good solubility in a wide range of solvents, especially water, which makes it hard to use widely in biosensing applications. Furthermore, graphene oxide (GO), as essentially a GR sheet derivatized which is the product of chemical exfoliation of graphite, possesses carboxylic acid, phenol hydroxyl and epoxide groups on the basal plane. The presence of oxygen functionalities on the GO surface is very helpful for cross-linking and/or entrapping enzymes [25,26]. In our earlier work [27], a novel GR-GO nanocomposite with many oxygen functionalities was prepared. Compared with GR, GR-GO has greater conductivity due to plenty of edge-plane-like defective sites that are beneficial for accelerating the electron transfer.

Herein, GOD was immobilized onto the surface of GR-GO without any fixing materials in this study. The DET of GOD was investigated using cyclic voltammetry (CV). The results demonstrated that a highly sensitive and simple electrochemical platform has been established, and possesses two advantages of effectively prevented the leakage of GOD and provided an attractive route to promote the electron transfer between GOD and electrode. As far as we know, the immobilization of GOD on GR-GO has never been reported in the literature.

2. EXPERIMENTAL

2.1. Reagents

Graphite was purchased from Kaitong Chemical Reagent Co., Ltd. (Tianjin, China). Graphene (prepared by chemical vapor deposition, CVD) was purchased from XF Nano Materials Co., Ltd.

(Nanjing, China). Glucose oxidase was obtained from Sangon Biotech Co., Ltd. (Shanghai, China) and used without further treatment. β -D-glucose was purchased from Tokyo Chemical Industry Co., Ltd. (Tokyo, Japan). All other chemicals were of analytical grade. The supporting electrolyte used in this work was phosphate-buffered solution (PBS), which was prepared by mixing stock solutions of 0.1 M KH_2PO_4 and 0.1 M K_2HPO_4 . The pH value of the PBS was adjusted from 4 to 10 by either 1 M KOH or 1 M H_3PO_4 . The solutions used in the whole work were prepared with doubly distilled water.

2.2. Apparatus

The electrochemical tests were obtained on a CHI660B electrochemical workstation (Chenhua, Shanghai). Three-electrode system which consisted of a bare or modified glassy carbon electrode (GCE) ($d=3$ mm) as the working electrode, a Pt wire and Ag/AgCl (saturated KCl) as the counter electrode and reference electrode was used in this study. According to the Randles-Sevcik equation, the effective surface area of the working electrodes was calculated by performing CVs with different scan rates in 1 mM $\text{K}_3\text{Fe}(\text{CN})_6$ (containing 0.1 M KCl) solution [28]. The CVs were carried out in 4.0 mL quiescent PBS solution at 100 mV s^{-1} and electrolytes in the electrochemical cell were kept in nitrogen (N_2) atmosphere (except during electrocatalysis of glucose).

2.3. Synthesis of the GR-GO nanocomposite

The GR-GO nanocomposite was prepared according to a previously published method [27]. Briefly, 10 mg GO and 25 mg GR were dispersed in 70 ml water by means of ultrasonic wave for 1h. Afterwards, the GR-GO nanocomposite was described as 0.5mg/mL until there was no visible precipitation. The dispersion was highly stable for months. For comparison purposes, GO and GR dispersions (0.5 mg/mL) were dissolved in water and dimethylformamide solvent, respectively.

2.4. Fabrication of the GR-GO-modified GCE and assembly of GOD

Prior to the electrode fabrication, the bare GCE was polished with 0.3 and 0.05 μm α -alumina slurries to obtain a mirror-like electrode, washed with ethanol and deionized water, and dried by blowing N_2 . The GR-GO/GCE was fabricated by pipetting 5 μL of GR-GO (0.5 mg/mL) onto the GCE and drying at room temperature.

GOD was assembled on the GR-GO nanocomposite by soaking the GR-GO/GCE in the GOD enzyme solution (20 mg/mL) at 4°C for 24 h. Thereafter, the electrode (denoted as GOD/GR-GO/GCE) was washed carefully with doubly distilled water to remove loosely adsorbed enzyme and stored at 4°C when not in use. For comparison, GOD/GCE, GOD/GO/GCE, and GOD/GR/GCE were prepared by adopting similar procedures.

3. RESULTS AND DISCUSSION

3.1. Electrochemical characterizations of the modified electrode

The four different working electrodes were evaluated with its conductivity by means of CV in $K_3[Fe(CN)_6]$ solution at scan rate of 100 mV s^{-1} . Fig. 1 shows the CV data of GCE (a), GO/GCE (b), GR/GCE (c), and GR-GO/GCE (d). On the bare GCE (Fig. 1a), the peak-to-peak spacing (ΔE_p) was 83 mV, which means that a reversible redox reaction was achieved. For GO/GCE, a couple of irreversible redox peaks appeared, and the peak current of redox significantly decreased, indicating the poor electrical conductivity of GO. As for GR/GCE and GR-GO/GCE, ΔE_p was approximately 71 mV and 67 mV respectively implying the faster electron transfer kinetics at the modified electrode. Evidently, there was a more enhanced redox currents on GR-GO/GCE compared to the bare GCE and the GR/GCE. This enhancement can be ascribed to the large surface area of GR/GO (the surface areas of GCE, GR/GCE, and GR-GO/GCE were 0.053 cm^2 , 0.066 cm^2 , and 0.085 cm^2 , respectively) and the plenty of various edge-plane-like defective sites that would be helpful to the electron transfer [27].

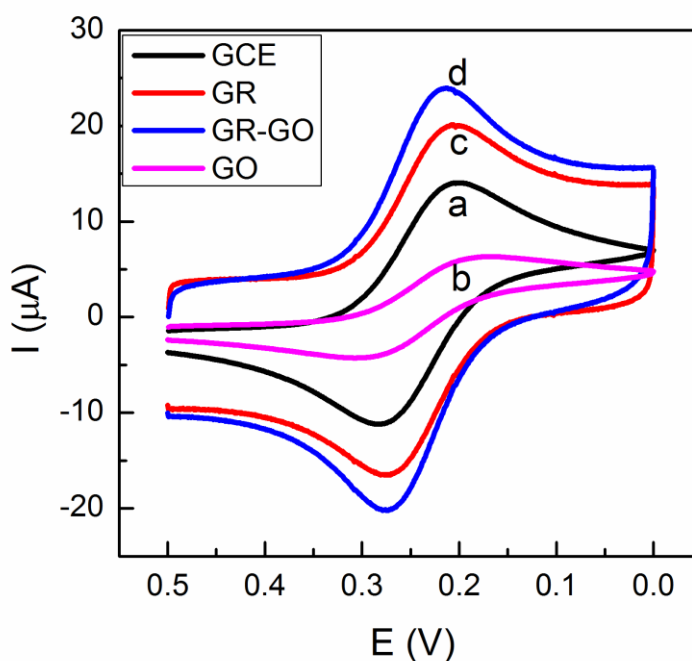


Figure 1. Cyclic voltammograms of GCE (a), GO/GCE (b) GR/GCE (c) and GR-GO/GCE (d) in 1 mM $K_3[Fe(CN)_6]$ containing 0.1 M KCl.

3.2. Direct electrochemistry of GOD

CV was performed to evaluate the electrochemical behavior of GOD on different modified electrodes. Fig. 2 shows the CVs of the GOD/GCE (a), GOD/GO/GCE (b), GOD/GR/GCE (c), and GOD/GR-GO/GCE (d) in N_2 -saturated 0.1 M pH 7.0 PBS at a scan rate of 100 mV s^{-1} . At the GOD/GCE, there was no redox peaks observed. This supports the fact that the direct electrochemistry of GOD was not achieved. At the same time, a similar results were also obtained for GOD/GO/GCE

due to the poor electrical conductivity of GO [26]. Significantly, at the GOD/GR-GO/GCE, there was a well defined and more enhanced redox current peaks. By averaging the anodic and cathodic peak potentials, the formal potential ($E^{0'}$) was calculated as -0.427V , which was close to the $E^{0'}$ value previously reported [4], attributed to the DET of GOD for the conversion of GOD (FAD) to GOD (FADH₂) [29].

The ratio of anodic and cathodic peak current (I_{pa}/I_{pc}) was approximately 1, and the ΔE_p was 41 mV, confirming that redox of GOD at GR-GO/GCE achieved at a fast electron transfer rate. It was ascribed to the presence of oxygen functionalities on the GR-GO surface that could easily bind with the free amino groups of GOD through covalent linkage [26, 30], and plenty of edge-plane-like defective sites on GR-GO nanocomposite. For comparison, the CV of GOD/GR/GCE was also measured. It was found that GOD/GR/GCE could also obtain DET of GOD. However, the current evidently decreased as GOD was weakly adsorbed onto GR, and no immobilizing agent was used [29]. Therefore, the leakage of some enzyme was inevitable.

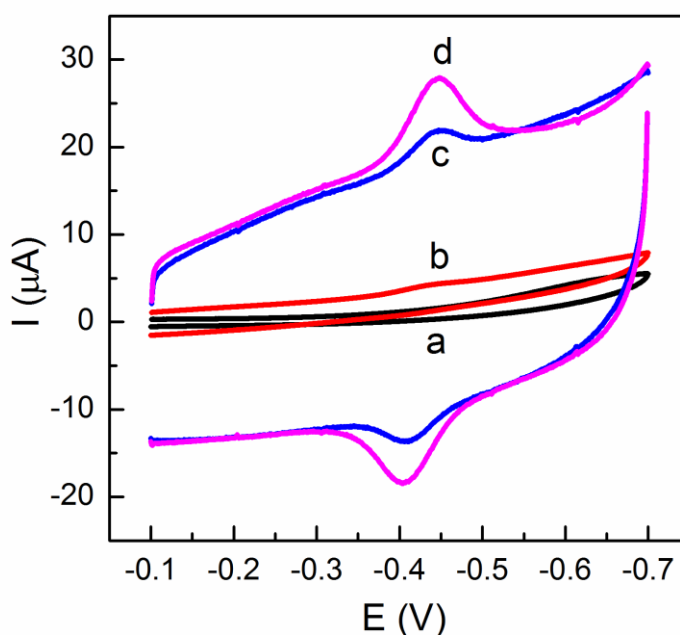


Figure 2. Cyclic voltammograms of GOD/GCE (a), GOD/GO/GCE (b), GOD/GR/GCE (c) and GOD/GR-GO/GCE (d) in N₂-saturated PBS (pH = 7.0).

3.3. Effect of pH

The influence of pH of the PBS on the direct electrochemistry of GOD at the GR-GO modified electrode was investigated, as shown in Fig. 3. The CV data with well-defined and stable redox peaks were observed over the pH range of 4.0–10.0. Apparently, the maximum peak current was obtained at pH 7.0, which was chosen as the proper pH. Moreover, a negative shift of both the cathodic and anodic peak potentials (E_{pc} , E_{pa}) occurred with the increasing of pH, indicating that the proton was directly involved in the electrochemical redox process. As can be seen in Fig. 3B, the E_{pa} and E_{pc} exhibited linear dependence with pH 4.0–10.0, and the regression equations could be expressed as: E_{pa} (V) =

$-0.0285 - 0.0515 \text{ pH}$ ($R = 0.997$) and $E_{pc} \text{ (V)} = -0.0884 - 0.0496 \text{ pH}$ ($R = 0.999$), respectively. The slopes of the two regression equations were close to the theoretical value of -58.6 mV/pH for an equal number of proton and electron transfer processes [31].

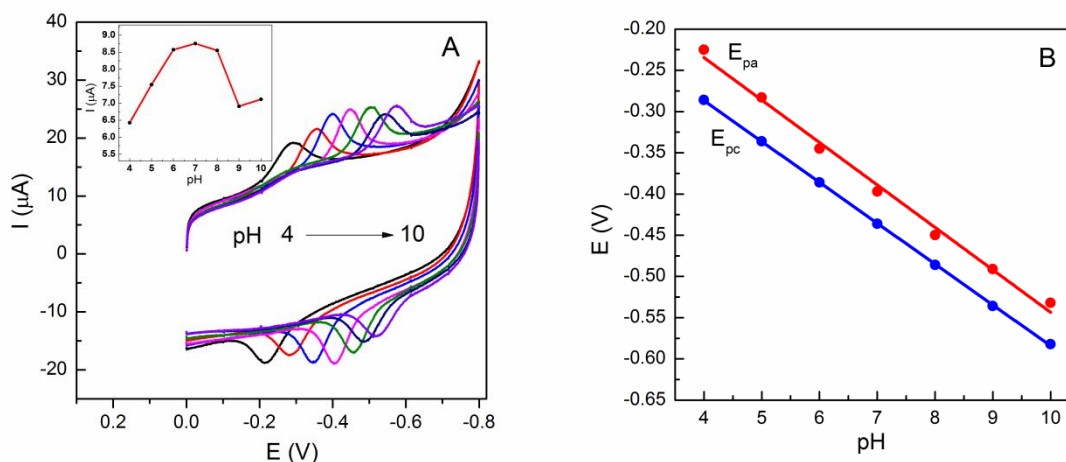


Figure 3. (A) Cyclic voltammograms of the GOD/GR-GO/GCE in N₂-saturated different pH PBS; Inset: effects of pH on the oxidation peak current (B) The plots of peak potentials vs. pH.

3.4. Effect of the scan rate

Fig.4 shows the CVs of GOD on GR-GO/GCE in deoxygenated PBS (pH 7.0) through a series of different scan rates. It is evident from Fig. 4A that the redox peak currents of GOD after background subtraction (performed using CV without GOD at the corresponding scan rate) increased with increasing scan rate from 10 to 500 mV s^{-1} . As can be seen in inset of Fig.4A, the good linear correlation between the redox peak currents versus scan rates revealed that the electron transfer was a surface-controlled process. The linear regression equations are obtained as follows: $I_{pa} = -1.1876 - 0.0606 \nu$ ($\mu\text{A}, \text{mV s}^{-1}, R = 0.9976$) and $I_{pc} = 1.1547 + 0.0580 \nu$ ($\mu\text{A}, \text{mV s}^{-1}, R = 0.9977$). Additionally, the amount of electroactive enzyme on the modified electrode surface (*I*) could be evaluated from the slope of the above linear regression equations by the following equation [32]:

$$I_p = n^2 F^2 \nu A \Gamma / 4RT \quad (1)$$

where *n* denotes the number of electrons transferred ($n = 2$), ν (V s^{-1}) denotes the scan rate, and *A* (cm^2) denotes the modified working electrode surface area. The constants *R*, *T*, and *F* have their usual meanings ($R = 8.314 \text{ J K}^{-1} \text{ mol}^{-1}$, $T = 298 \text{ K}$, $F = 96485 \text{ C mol}^{-1}$). The amount of electroactive GOD was calculated to be $2.69 \times 10^{-10} \text{ mol cm}^{-2}$, which was higher than that of GOD/RGO/GCE, at $1.22 \times 10^{-10} \text{ mol cm}^{-2}$ [26], and the GOD/poly(ViBuIm⁺Br⁻)-G/GC electrode, at $1.45 \times 10^{-11} \text{ mol cm}^{-2}$ [33], indicating that the GR-GO prepared in this work was very beneficial for GOD immobilization.

The relationship between peak potentials and the logarithm of scan rates ($\log \nu$) were shown in Fig.4B. As can be seen in inset of Fig.4B, the *E*_{pa} and *E*_{pc} were linearly proportional to the $\log \nu$ at high scan rate. With $2.3RT/(1 - \alpha)nF$ and $2.3RT/\alpha nF$ for the slopes of the regression equations, the value of α (charge transfer coefficient) was calculated to be 0.52. Based on the Laviron equation [34], the electron transfer rate constant (*k*_s) can be further calculated as follows:

$$\log k_s = \alpha \log(1 - \alpha) + (1 - \alpha) \log \alpha - \log(RT/nFv) - \alpha(1 - \alpha)nF\Delta E_p/2.3RT \quad (2)$$

where α was 0.52 and all the other parameters were standard values. The k_s value was calculated to be 3.5 s^{-1} , which was larger than those of other graphene-modified electrodes, such as GOD/graphene-chitosan/GCE (2.83 s^{-1}) [17], GOD-graphene/GCE (2.68 s^{-1}) [18], and GOD/PDDA-G/GCE (1.59 s^{-1}) [35]. The results confirmed that the GCE modified with GR-GO with more effective surface area and active point enabled fast DET between FAD and the electrode.

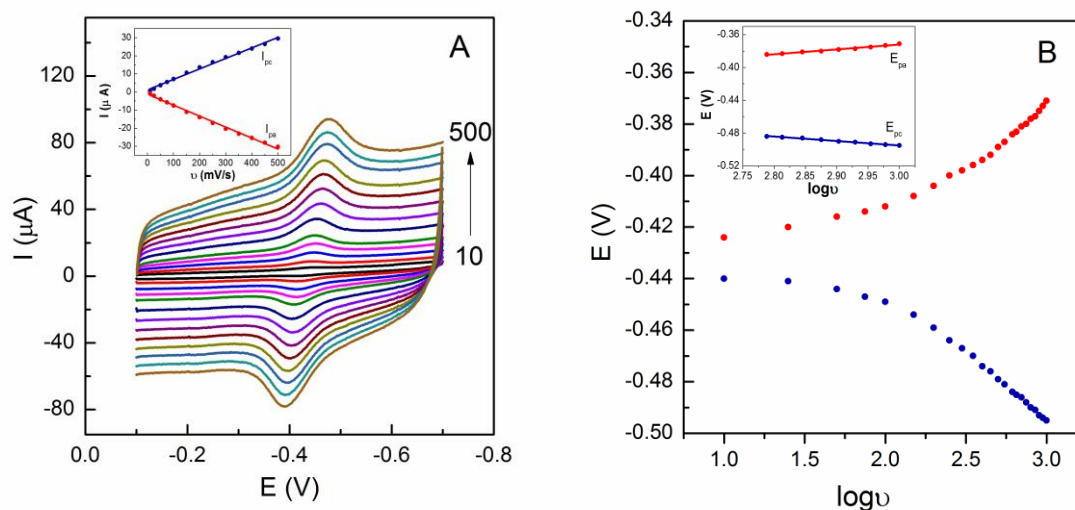
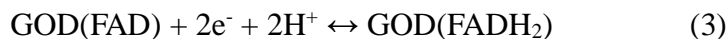


Figure 4. (A) Cyclic voltammograms of GOD/GR-GO/GCE in N₂-saturated PBS (pH 7.0) at different scan rates (from inner to outer: 10, 50, 100, 150, 200, 250, 300, 350, 400, 450 and 500 mV s⁻¹). Inset: linear dependence of I_{pa} and I_{pc} on scan rates. (B) The relationship of the peak potentials vs. the logarithm of scan rate (log ν) from 10 to 1000 mV s⁻¹. Inset: the linear fitting section from 600 to 1000 mV s⁻¹.

3.5. Electrocatalytic behavior of GOD/GR-GO/GCE towards O₂ and glucose determination

Fig. 5 shows the CV data for the GOD-GR-GO/GCE in N₂ (curve a), air (curve b), and O₂ (curve d)-saturated PBS at the scan rate of 100 mV s⁻¹. The electrocatalytic process can be expressed as follows [19]:



Due to the fast electron transfer on the modified electrode surface, the DET of GOD in PBS saturated with N₂ could achieve the conversion from GOD(FAD) to GOD(FADH₂) (Eq. 3). Then, GOD(FADH₂) was oxidized to GOD(FAD) by dissolved oxygen (Eq. 4), and the regenerated oxidized form of GOD(FAD) enhanced the cathodic peak current. The curve c shows that with the increment of glucose content, the reduction peak current would decrease. This indicated that the addition of glucose to the reaction system reduced the concentration of GOD(FAD) (Eq. 5), leading to the decrease in cathodic current.



Therefore, based on the decrease in the reduction current caused by the addition of glucose, the proposed GOD/GR-GO/GCE can be used as a glucose biosensor.

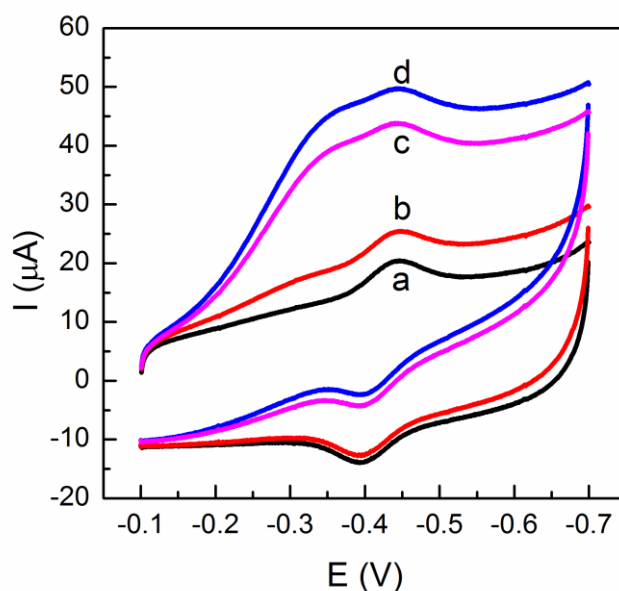


Figure 5. Cyclic voltammograms of GOD/GR-GO/GCE in (a) N_2 -saturated PBS, (b) air-saturated PBS, (c) O_2 -saturated PBS with addition of 2 mM glucose and (d) O_2 -saturated PBS.

Fig. 6 shows the CV data for the GOD/GR-GO/GCE in O_2 -saturated PBS with different concentrations of glucose. In reaction systems added glucose with different concentration, there was obvious linear relationship between the concentration of glucose and reduction peak current at a certain limit ranging from 0.1 to 11 mM (inset of Fig. 6). The linear regression equation was $I_{pc} = 22.1586 - 0.9506c$ (μA , mM, $R = 0.996$). The detection limit of the biosensor was estimated to be 20 μM ($S/N=3$). The sensitivity of the GOD/GR-GO/GCE was $15.85 \mu A mM^{-1} cm^{-2}$, much higher than those previously reported, for example, RGO-GOD/GCE ($1.85 \mu A mM^{-1} cm^{-2}$) [26] and GOD/ERGO/GCE ($6.82 \mu A mM^{-1} cm^{-2}$) [3]. Besides, the Michaelis-Menten constant (K_m), which can reveal the enzyme-substrate reaction kinetics, was further estimated to be 1.23 mM using the Lineweaver-Burk equation [36]. The lower magnitude of K_m confirmed the retention of the GOD native structure in GOD/GR-GO/GCE, resulting in higher affinity and activity of GOD toward glucose in an enzymatic reaction. All these conclusions showed that this prepared glucose biosensor was suitable for its practical application.

The sensing performance of this work is compared with some reported sensors in the literature as shown in Table 1 [4, 37-42]. As could be seen, the glucose sensor we proposed have a wider linear response range or lower detection limit than the sensors fabricated by the MWCNT-chitosan [37], graphene-CdS [38], Nafion-mesocellular graphene foam [39], rGO-Ag [4], rGO-Ag-titanium dioxide nanotube [40], Carbon nanotubes-GO [41] composites. Moreover, the GR-GO nanocomposite modified electrode was comparable with Ag-GO-ZnO-chitosan [42], but it was a simple-fabricated material compared with the complex synthesis of Ag-GO-ZnO-chitosan.

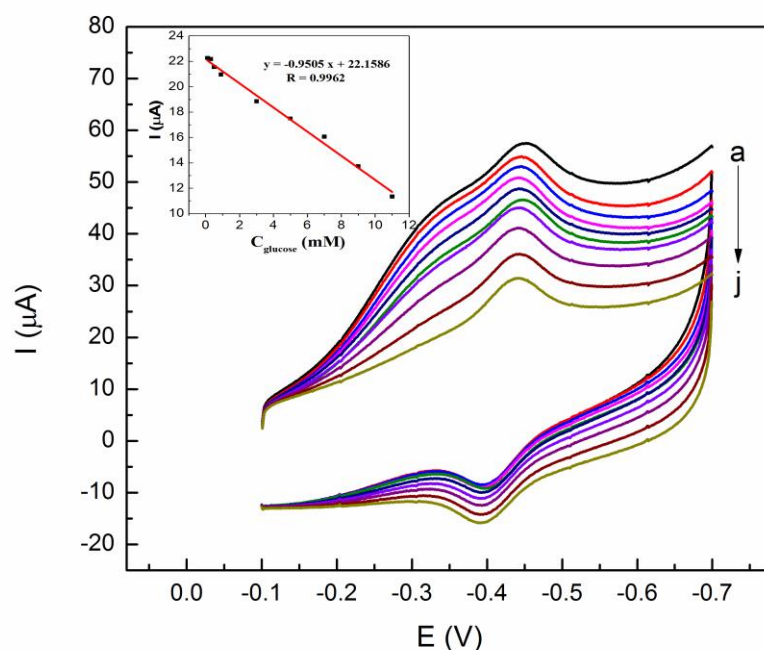


Figure 6. Cyclic voltammograms of GOD/GR-GO/GCE in O_2 saturated PBS (pH 7.0) containing various concentrations of glucose (a) 0, (b) 0.1, (c) 0.3, (d) 0.5, (e) 1, (f) 3, (g) 5, (h) 7, (i) 9 and (j) 11 mM. The inset shows the linear dependence of I_{pc} over glucose concentrations.

Table 1. The comparison of this work with other glucose biosensors

Electrode	Detection limit (μM)	Linear range (mM)	Reference
MWCNT-chitosan	20	1.0-10.0	[37]
graphene-CdS	700	2.0-16.0	[38]
Nafion-mesocellular graphene foam	250	1.0-12	[39]
rGO-Ag	160	0.5-12.5	[4]
rGO-Ag-titanium dioxide nanotube	2.2	5-15.5	[40]
Carbon nanotubes-GO	28	0.05-23.2	[41]
Ag-GO-ZnO-chitosan	10.6	0.1-12	[42]
This work	20	0.1-11	

3.6. Reproducibility, repeatability, and stability of the biosensor

In order to investigate the reproducibility of the biosensor, five identical electrodes were prepared for determination of 5 mM glucose under the same conditions, and the RSD was 4.56%. The result indicated that the biosensor own appreciable reproducibility. Furthermore, six successive tests were carried out in 1 mM glucose, and the RSD was 1.17%, which implied that the biosensor own a

good repeatability [43, 44]. After the biosensor was stored at 4°C under dry conditions for one week, the current response was approximately 95% of its original value. Such a high stability could be attributed to the good biocompatibility of the GR-GO nanocomposite and effective immobilization of GOD.

3.7 Selectivity study and real sample analysis

In order to investigate the selectivity of the biosensor, the common biological active substances such as dopamine, uric acid, and ascorbic acid was test in oxygenated PBS. It was found that the addition of 0.1 mM of interferents did no noteworthy response for the determination of 1 mM glucose. Obviously, the biosensor has a high selectivity.

In order to investigate the possible application of the developed biosensor in clinical analysis, the GOD/GR-GO/GCE was utilized to detect glucose in human serum and human urine samples. Based on this study, the glucose concentration in blood was found to be 4.90 mM, which was close to the standard value of 4.98 mM determined by a spectrophotometric method on a standard clinical laboratory. There was no target analytes in human urine samples. The standard solution was added to the samples to determine the recovery rate, and the results were summarized in Table 2. As can be seen, the recoveries for glucose in serum and urine sample were 95.5-103.2% and 98.4-102.8%. The results demonstrated good accuracy for the determination of glucose in real samples.

Table 2. Determination of glucose in serum and urine sample.

Samples	Added(mM)	Found(mM)	Recover rate(%)
serum	0.0	1.17	-
	1.0	2.07	95.5
	2.0	3.23	101.8
	5.0	6.37	103.2
	urine	2.0	2.02
	3.0	2.95	98.4
	4.0	4.11	102.8
	5.0	5.04	100.8

4. CONCLUSIONS

In this work, we achieved the direct electrochemistry for GOD by employing a GR-GO nanocomposite without any cross-linker. The modified electrode exhibited high electrocatalytic activity towards glucose determination via oxygen consumption. The results indicated that the GR-GO nanocomposite provided a favorable microenvironment for the enzyme and promoted the direct electron transfer at the electrode surface. Excellent analytical performances were achieved with the fabricated biosensor, as well as appreciable storage and operational stabilities. Because of its wide linear range, fast electron transfer rate, high selectivity, and good stability, the practical applications of this sensor can be further extended.

ACKNOWLEDGEMENTS

This work was financially supported by the Natural Science Foundation of Hebei Province (No.B2016109028) and Foundation of Hebei Education Department (No. ZC2016068).

References

1. J. Tkac, P. Vostior Gemeiner, E. Sturdik, *J. Bioelectrochemistry*, 56 (2002) 127.
2. L.C. Clark Jr., C. Lyons, Ann. N. Y. Acad, *Science*, 102 (1962) 29.
3. M. Cui, B. Xu, C.G. Hu, H.B. Shao, L.T. Qu, *Electrochim. Acta*, 98 (2013) 48.
4. S. Palanisamy, C. Karuppiah, S.M. Chen, *Colloids Surf. B.*, 114 (2014) 164.
5. J.T. Holland, C. Lau, S. Brozik, P. Atanassov, S. Banta, *J. Am. Chem. Soc.*, 133 (2011) 19262.
6. C.Y. Deng, J.H. Chen, Z. Nie, S.H. Si, *Biosens. Bioelectron.*, 26 (2010) 213.
7. Q. Xu, S.X. Gu, Y.E. Zhou, Z.J. Yang, W. Wang, X.Y. Hu, *Sens. Actuators. B.*, 190 (2014) 562.
8. T. Kuwahara, K. Ogawa, D. Sumita, M. Kondo, M. Shimomura, *J. Electroanal. Chem.*, 811 (2018) 62.
9. J.P. Li, Y.P. Li, Y. Zhang, G. Wei, *Anal. Chem.*, 84 (2012) 1888.
10. A. Salimi, E. Sharifi, A. Noorbakhsh, S. Saied, *Biosens. Bioelectron.*, 22 (2007) 3146.
11. D. Patil, N.Q. Dung, H. Jung, S.Y. Ahn, D.M. Jang, D. Kim, *Biosens. Bioelectron.*, 31 (2012) 176.
12. Y.Y. Wei, Y. Li, X.Q. Liu, Y.Z. Xian, G.Y. Shi, L.T. Jin, *Biosens. Bioelectron.*, 26 (2010) 275.
13. K.S. Galhardo, R.M. Torresi, S.I.C. Torresi, *Electrochim. Acta*, 73 (2012) 123.
14. X.J. Chen, J.W. Zhu, R. Tian, C. Yao, *Sens. Actuators. B.*, 163 (2012) 272.
15. C. J. Kim, X. Wang, J. H. Kim, S. B. Kim, H. H. Kim, *New Biotechnol.*, 44(2018) s97.
16. R.J. Cui, Z.D. Han, J. Pan, E.S. Abdel-Halim, J.J. Zhu, *Electrochim. Acta*, 58 (2011) 179.
17. C. I. L. Justino, A. R. Gomes, A. C. Freitas, A. C. Duarte, T. A. P. Rocha-Santos, *TrAC, Trends Anal. Chem.*, 91 (2017) 53.
18. P. Wu, Q. Shao, Y.J. Hu, J. Jin, Y.J. Yin, H. Zhang, C.X. Cai, *Electrochim. Acta*, 55 (2010) 8606.
19. J.N. Hui, J.W. Cui, G.Q. Xu, S.B. Adeloju, Y.C. Wu, *Mater. Lett.*, 108 (2013) 88.
20. W. Grosse, J. Champavert, S. Gambhir, G.G. Wallace, S.E. Moulton, *Carbon*, 61 (2013) 467.
21. K.S. Novoselov, A.K. Geim, S.V. Morozov, D. Jiang, Y. Zhang, S.V. Dubonos, I.V. Grigorieva, A.A. Firsov, *Science*, 306 (2004).
22. F. N.I. Sari, J. M. Ting, *Surf. Coat. Technol.*, 303 (2016) 176.
23. J. Rao, R. Xu, T. Zhou, D. Zhang, C. Zhang, *J. Alloys Compd.*, 728 (2017) 376.
24. M. Yoonessi, Y. Shi, D.A. Scheiman, M.L. Colon, D.M. Tigelaar, R. A. Weiss, M.A. Meador, *ACS Nano*, 6 (2012) 7644.
25. Y. Liu, D.S. Yu, C. Zeng, Z.C. Miao, L.M. Dai, *Langmuir*, 26 (2010) 6158.
26. B. Unnikrishnan, S. Palanisamy, S.M. Chen, *Biosens. Bioelectron.*, 39 (2013) 70.
27. X.B. Zhou, Z.F. He, Q.W. Lian, Z. Li, H. Jiang, X.Q. Lu, *Sens. Actuators, B.*, 193 (2014) 198.
28. S.F. Wang, F. Xie, R.F. Hu, *Anal. Bioanal. Chem.*, 387 (2007) 933.
29. C. Shan, H. Yang, J. Song, D. Han, A. Ivaska, L. Niu, *Anal. Chem.*, 81 (2009) 2378.
30. S. Alwarappan, C. Liu, A. Kumar, C.Z. Li, *J. Phys. Chem. C.*, 114 (2010) 12920.
31. Q. Xu, S.X. Gu, L.Y. Jin, Y.E. Zhou, Z.J. Yang, W. Wang, X.Y. Hu, *Sens. Actuators. B.*, 190 (2014) 562.
32. V. Mani, B. Devadas, S.M. Chen, *Biosens. Bioelectron.*, 41 (2013) 309.
33. Q. Zhang, S.Y. Wu, L. Zhang, J. Lu, F. Verproot, Y. Liu, Z.Q. Xing, J.H. Li, X.M. Song, *Biosens. Bioelectron.*, 26 (2011) 2632.
34. E. Laviron, *J. Electroanal. Chem. Interfacial Electrochem.*, 101 (1979) 19.
35. L.P. Jia, J.F. Liu, H.S. Wang, *Electrochim. Acta*, 111 (2013) 411.
36. H. Razmi, R.M. Rezaei, *Biosens. Bioelectron.*, 41 (2013) 498.
37. C. Yang, C. Xu and X. Wang, *Langmuir*, 28 (2012) 4580.
38. Y. Wang, L. Liu, M. Li, S. Xu and F. Gao, *Biosens. Bioelectron.*, 30 (2011) 107.

39. Y. Wang, H.X. Li and J.L. Kong, *Sens. Actuators, B.*, 193 (2014) 708.
40. W. Wang, Y. Xie, C. Xia, H. Du, F. Tian, *Microchim. Acta*, 181 (2014) 1325.
41. S. Palanisamy, S. Cheemalapati, S.M. Chen, *Mater. Sci. Eng. C.*, 34 (2014) 207.
42. Z. Li, L. Sheng, A. Meng, C. Xie, K. Zhao, *Microchim. Acta*, 183 (2016) 1625.
43. S.M. Naghib, E. Parnian, H. Keshvari, E. Omidinia, M. Eshghan-Malek, *Int. J. Electrochem. Sci.*, 13 (2018) 1013
44. A.A. Ismail, A.M. Ali, F.A. Harraz, M. Faisal, H. Shoukry, A.E. Al-Salami, *Int. J. Electrochem. Sci.*, 14 (2019) 15

© 2019 The Authors. Published by ESG (www.electrochemsci.org). This article is an open access article distributed under the terms and conditions of the Creative Commons Attribution license (<http://creativecommons.org/licenses/by/4.0/>).